

# Dynamic Behaviour of the [(Triphos)Rh( $\eta^1:\eta^2$ -P<sub>4</sub>RR')]<sup>n+</sup> Complexes [Triphos = MeC(CH<sub>2</sub>PPh<sub>2</sub>)<sub>3</sub>; R = H, Alkyl, Aryl; R' = Lone Pair, H, Me; n = 0, 1]: NMR and Computational Studies

Pierluigi Barbaro,<sup>[a]</sup> Maria Caporali,<sup>[a]</sup> Andrea Ienco,<sup>[a]</sup> Carlo Mealli,<sup>[a]</sup>  
Maurizio Peruzzini,<sup>\*,[a]</sup> and Francesco Vizza<sup>[a]</sup>

**Keywords:** Phosphorus / Rhodium / Tripodal phosphane ligands / Fluxionality / Density functional calculations / NMR spectroscopy

Solution multinuclear and multidimensional NMR analyses of the [(triphos)Rh( $\eta^1:\eta^2$ -P<sub>4</sub>RR')]<sup>n+</sup> complex cations [triphos = MeC(CH<sub>2</sub>PPh<sub>2</sub>)<sub>3</sub>; R = H, Me, Ph; R' = lone pair, H, Me; n = 0, 1] confirm the same primary structure determined by X-rays in the solid state. In addition, 2D <sup>1</sup>H NOESY and <sup>31</sup>P{<sup>1</sup>H} exchange NMR spectroscopy show that these complexes are nonrigid on the NMR time-scale over the 253–318 K temperature range. A dynamic process that involves the terminal phosphane groups of the triphos ligand is displayed by each compound. The NMR spectroscopic data indicate a slow

scrambling motion in which the P<sub>4</sub>R unit tumbles with respect to the (triphos)Rh moiety. DFT calculations outline a possible turnstile mechanism involving the threefold and twofold rotors into which the complex is subdivided. The process goes through a transition state in which the axial and equatorial dispositions of the PRR' and P=P donating groups of the P<sub>4</sub>RR' ligand are inverted with respect to the ground state.

(© Wiley-VCH Verlag GmbH & Co. KGaA, 69451 Weinheim, Germany, 2008)

## Introduction

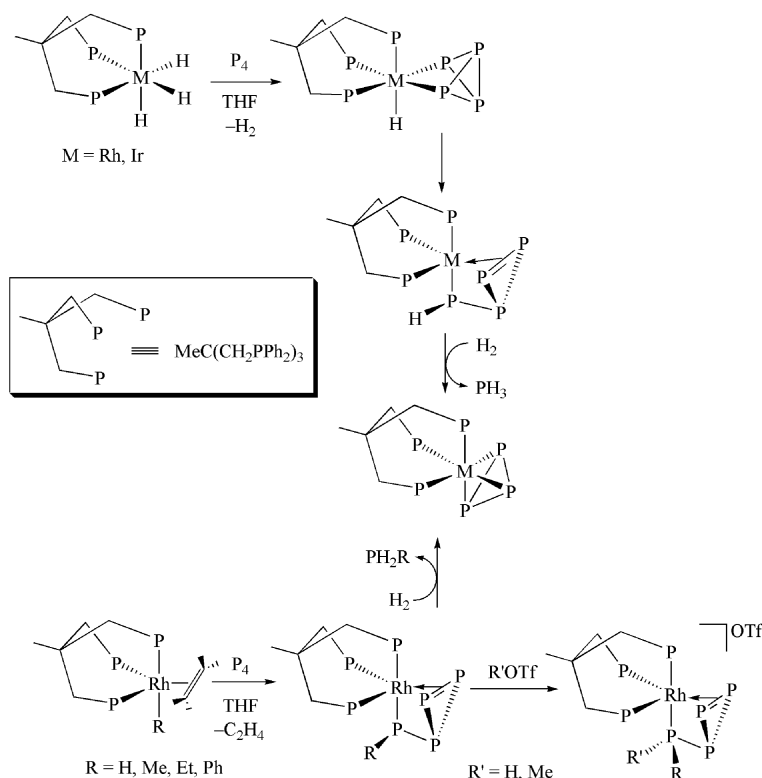
White phosphorus is a cheap chemical largely used in the manufacturing of organophosphorus compounds.<sup>[1]</sup> These industrially important derivatives are generally produced by the reaction of PCl<sub>3</sub> or PCl<sub>5</sub> with suitable organic reagents. The industrial process is not very environmentally sustainable as the reaction involves gaseous chlorine and releases huge amounts of hydrochloric acid into the atmosphere. Therefore, the discovery of new and efficient methods for the preparation of organophosphorus derivatives from P<sub>4</sub> through non-chlorine routes remains a challenging task for the industry.<sup>[2]</sup> Moreover, the underpinnings of the formation of P–C and P–H bonds need to be understood in more detail.<sup>[2,3]</sup> Advances in this area entail the use of transition metal systems that are suitable for the activation of both the P<sub>4</sub> tetrahedron and the organic substrate. On the other hand, a recent breakthrough in the area has been presented by Bertrand et al. who have reported on the reactivity of alkyl amino carbenes with P<sub>4</sub>. This process does not lead to the formation of any metal intermediate and leads to very reactive P–C bonds.<sup>[4]</sup>

Another important advancement in P<sub>4</sub> activation/functionalization was our previous finding that some rhodium

and iridium organometallic complexes containing the tripodal ligand, MeC(CH<sub>2</sub>PPh<sub>2</sub>)<sub>3</sub> (triphos), can activate the P<sub>4</sub> molecule and selectively deliver to it the hydride,<sup>[5]</sup> alkyl or aryl<sup>[6,7]</sup> ligand originally coordinated to the metal. Scheme 1 reports the highlights of this chemistry and, in particular, the reaction of [(triphos)MH<sub>3</sub>] (M = Rh, Ir) and [(triphos)-RhR(C<sub>2</sub>H<sub>4</sub>)] (R = H, alkyl, aryl) with P<sub>4</sub> to yield [(triphos)-M( $\eta^1:\eta^2$ -P<sub>4</sub>R)] compounds featuring a P–H or a P–C bond. Direct alkylation of the rhodium derivatives affords cationic species of the [(triphos)Rh( $\eta^1:\eta^2$ -P<sub>4</sub>RR')]<sup>+</sup> type, which can be isolated as solids. These were characterized in both the solid and solution states.<sup>[7]</sup>

These complexes are not only suitable organometallic platforms with which to study the transformation of P<sub>4</sub> into organophosphorus compounds,<sup>[8]</sup> but are also intriguing for their structural and bonding properties. In particular, because of their lack of molecular symmetry, these species exhibit a complicated <sup>31</sup>P NMR splitting pattern resulting from the presence of eight different NMR-active nuclei (ABCDEFGX spin system). Polyphosphorus ligands usually exhibit interesting NMR properties and often show a fluxional behaviour, which can be related to different processes such as scrambling of coordinated ligands,<sup>[9]</sup> skeleton rearrangements<sup>[10]</sup> and rotational interconversions.<sup>[11]</sup> Since the triphos complexes formed by polyphosphorus units such as *cyclo*-P<sub>3</sub><sup>[12]</sup> or *cyclo*-P<sub>2</sub>X (X = S, Se, Te)<sup>[13]</sup> exhibit an overall fluxionality due to both the triphos and the naked polyphosphorus unit, it is not surprising that the [(triphos)-

[a] Consiglio Nazionale delle Ricerche, Istituto di Chimica dei Composti OrganoMetallici,  
Via Madonna del Piano 10, 50019 Sesto Fiorentino, Firenze, Italy  
E-mail: maurizio.peruzzini@iccom.cnr.it



Scheme 1. Summary of the reactivity of [(triphos)MH<sub>3</sub>] (M = Rh, Ir) and [(triphos)RhR(C<sub>2</sub>H<sub>4</sub>)] (R = H, Me, Et, Ph) with P<sub>4</sub>.

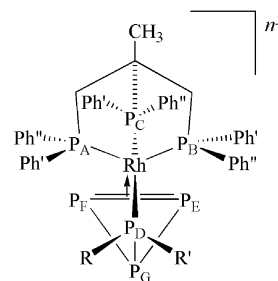
M( $\eta^1$ : $\eta^2$ -P<sub>4</sub>R)] and [(triphos)M( $\eta^1$ : $\eta^2$ -P<sub>4</sub>RR')]<sup>n+</sup> complexes also lack stereochemical rigidity in solution. Remarkably, the occurrence of a fluxional behaviour in these species could not be evinced from the inspection of the room temperature spectra, but became evident from the observation of inverted-phase peaks in the <sup>1</sup>H NOESY NMR spectra. This unexpected observation, which was also confirmed by variable-temperature NMR measurements, prompted us to study in detail the dynamic behaviour of these complexes. In this work, which combines experimental NMR spectroscopic data and DFT modelling, a mechanistic picture of the observed dynamic process is presented.

## Results and Discussion

### Dynamic Behaviour of the [(Triphos)Rh( $\eta^1$ : $\eta^2$ -P<sub>4</sub>RR')]<sup>n+</sup> Complexes in Solution: NMR Studies

The solid- and solution-state structures of the [(triphos)Rh( $\eta^1$ : $\eta^2$ -P<sub>4</sub>R)] [R = H (**1**), Me (**2**), Et (**3**), Ph (**4**)] and [(triphos)Rh( $\eta^1$ : $\eta^2$ -P<sub>4</sub>RR')](OTf) [R = H, R' = Me (**5**); R = Ph, R' = Me (**6**); OTf = OSO<sub>2</sub>CF<sub>3</sub>] Rh<sup>I</sup> complexes were previously obtained from detailed multinuclear and multidimensional NMR analysis and, for **6**, from X-ray diffraction. In both complexes, the same primary structure is retained.<sup>[7]</sup>

As shown in Scheme 2, which also indicates the labelling scheme adopted for the NMR assignments, the coordination geometry around the metal is best described as trigonal bipyramidal (TBP) rather than pseudo-octahedral. In fact, the P<sub>4</sub>RR' unit may be considered to be acting as a bidentate ligand in which a P=P double bond in the P<sub>3</sub> ring occupies an equatorial position and the PRR'  $\sigma$ -donor group resides in an axial position. The coordination sphere at the



	R	R'	n	
1	H	<i>lp</i>	0	[(triphos)Rh( $\eta^1$ : $\eta^2$ -P <sub>4</sub> H)]
2	Me	<i>lp</i>	0	[(triphos)Rh( $\eta^1$ : $\eta^2$ -P <sub>4</sub> Me)]
3	Et	<i>lp</i>	0	[(triphos)Rh( $\eta^1$ : $\eta^2$ -P <sub>4</sub> Et)]
4	Ph	<i>lp</i>	0	[(triphos)Rh( $\eta^1$ : $\eta^2$ -P <sub>4</sub> Ph)]
5	Me	H	1	[(triphos)Rh( $\eta^1$ : $\eta^2$ -P <sub>4</sub> MeH)] <sup>+</sup>
6	Ph	Me	1	[(triphos)Rh( $\eta^1$ : $\eta^2$ -P <sub>4</sub> PhMe)] <sup>+</sup>

Scheme 2. Sketch of the [(triphos)Rh( $\eta^1$ : $\eta^2$ -P<sub>4</sub>RR')]<sup>n+</sup> complexes **1–6** showing the labelling scheme adopted for the NMR assignments; *lp* = lone pair.

rhodium centre is completed by the triphos P atoms occupying one axial and two equatorial positions. The bonding features of the [(triphos)M( $\eta^1$ : $\eta^2$ -P<sub>4</sub>RR')]<sup>n+</sup> (*n* = 0, 1) complexes compare well to those of the classic L<sub>4</sub>M( $\eta^2$ -olefin) ones.<sup>[7]</sup> In fact, the P=P double bond (localized at one side of the P<sub>3</sub> triangle) replaces the  $\eta^2$ -coordinated olefin ligand. Four other P  $\sigma$  donors—three from the triphos ligand and one from the PRR' unit—confer the typical butterfly shape to the supporting metal fragment of the L<sub>4</sub>M fragment (M = d<sup>8</sup>).

NMR experiments to determine the solution-state structure of this class of compounds were carried out by observing the <sup>1</sup>H, <sup>31</sup>P and <sup>13</sup>C signals over the 253–318 K temperature range in CD<sub>2</sub>Cl<sub>2</sub> or [D<sub>8</sub>]THF solutions. In each complex, all the <sup>31</sup>P, <sup>1</sup>H and <sup>13</sup>C nuclei are chemically non-equivalent because of the lack of any symmetry elements in the molecules. Only the protons of the terminal methyl group in triphos, as well as the *ortho* and *meta* proton pairs on the same phenyl ring, appear equivalent on the NMR time-scale; this is because of the fast rotation of the triphos methyl group and the phenyl groups around the C–C and C–P bonds, respectively. The phosphorus atoms of triphos in a pseudo-*trans* disposition to the P<sub>E</sub>, P<sub>F</sub> and P<sub>D</sub> phosphorus atoms of the P<sub>4</sub>RR' unit were labelled as P<sub>A</sub>, P<sub>B</sub> and P<sub>C</sub>, respectively. A higher chemical shift was arbitrarily assigned to P<sub>A</sub> than to P<sub>B</sub>. All the <sup>1</sup>H, <sup>31</sup>P and <sup>13</sup>C NMR resonances in 1–6 (Table 1 and Table 2) were unambiguously assigned by a combination of 1D and 2D NMR techniques (see Exp. Sect.).<sup>[7]</sup>

Table 1. <sup>31</sup>P{<sup>1</sup>H} NMR chemical shifts for the [(triphos)Rh( $\eta^1$ : $\eta^2$ -P<sub>4</sub>RR')]<sup>n+</sup> complexes.<sup>[a]</sup>

Nucleus	Complex					
	1 <sup>[b]</sup>	2 <sup>[b]</sup>	3 <sup>[c]</sup>	4 <sup>[d]</sup>	5 <sup>[c]</sup>	6 <sup>[e,f]</sup>
P <sub>A</sub>	15.96	15.61	12.49	13.86	15.88	15.91
P <sub>B</sub>	2.81	−1.94	−2.44	−12.03	9.75	2.56
P <sub>C</sub>	−10.78	−11.77	−11.42	−4.63	5.21	9.46
P <sub>D</sub>	−280.22	−214.08	−192.91	−213.44	−172.02	−156.75
P <sub>E</sub>	−180.12	−174.52	−178.24	−181.09	−190.11	−200.77
P <sub>F</sub>	−184.98	−198.79	−199.92	−201.39	−209.25	−174.04
P <sub>G</sub>	−3.33	26.79	24.28	18.14	5.60	17.39

[a] 202.46 MHz, [D<sub>8</sub>]THF, in ppm. [b] 293 K. [c] 253 K. [d] 266 K. [e] CD<sub>2</sub>Cl<sub>2</sub>. [f] 275 K; data from ref.<sup>[7]</sup>.

<sup>1</sup>H NOESY experiments were carried out on all complexes in order to obtain their structural characterization in solution. The <sup>1</sup>H NOESY spectra showed that, under the adopted experimental conditions, the *extreme narrowing limit* ( $\tau_c\omega_L \ll 1$ ) is attained by each compound. Indeed, with the exception of complex 5, only positive (negatively phased) NOEs were observed at 253 K.<sup>[14,15]</sup> Remarkably, apart from providing relevant structural information, the <sup>1</sup>H NOESY experiments showed that all of the examined complexes are not rigid on the NMR time-scale. In fact, strong positively phased <sup>1</sup>H exchange cross-peaks were observed, which is consistent with a slow exchange motional regime. In particular, the following selective exchange pathway for the *ortho*, *meta* and *para* protons of the triphos ligand was

Table 2. Selected <sup>1</sup>H NMR chemical shifts for the [(triphos)-Rh( $\eta^1$ : $\eta^2$ -P<sub>4</sub>RR')]<sup>n+</sup> complexes.<sup>[a]</sup>

Complex	Proton	$\delta$ <sup>[b]</sup>
1 <sup>[c]</sup>	P <sub>D</sub> H	0.01 (br. dd)
2 <sup>[c]</sup>	P <sub>D</sub> CH <sub>3</sub> (3 H)	0.65 (br. s)
3 <sup>[d]</sup>	P <sub>D</sub> CH <sub>2</sub> CH <sub>3</sub> (3 H)	0.70 (q)
	P <sub>D</sub> CH'	1.42
	P <sub>D</sub> CH''	0.30
4 <sup>[e]</sup>	<i>o</i> -PhP <sub>D</sub> (2 H)	7.66 (br. d)
	<i>o</i> -Ph'P <sub>A</sub> (2 H)	5.71 (t)
	<i>o</i> -Ph''P <sub>A</sub> (2 H)	8.12 (t)
	<i>o</i> -Ph'P <sub>B</sub> (2 H)	8.48 (t)
	<i>o</i> -Ph''P <sub>B</sub> (2 H)	8.09 (t)
	<i>o</i> -Ph'P <sub>C</sub> (2 H)	6.47 (t)
	<i>o</i> -Ph''P <sub>C</sub> (2 H)	7.33 (t)
5 <sup>[e]</sup>	P <sub>D</sub> CH <sub>3</sub> (3 H)	0.82 (br. s)
	P <sub>D</sub> H	3.50 (br. d)
6 <sup>[f,g]</sup>	P <sub>D</sub> CH <sub>3</sub> (3 H)	0.93 (br. d)
	<i>o</i> -PhP <sub>D</sub> (2 H)	8.01 (t)
	<i>o</i> -Ph'P <sub>A</sub> (2 H)	6.23 (dd)
	<i>o</i> -Ph''P <sub>A</sub> (2 H)	8.50 (t)
	<i>o</i> -Ph'P <sub>B</sub> (2 H)	8.21 (br.)
	<i>o</i> -Ph''P <sub>B</sub> (2 H)	6.66 (t)
	<i>o</i> -Ph'P <sub>C</sub> (2 H)	6.06 (t)
	<i>o</i> -Ph''P <sub>C</sub> (2 H)	7.49 (t)

[a] 500.132 MHz, solvent [D<sub>8</sub>]THF, signals are multiplets unless otherwise specified: s = singlet, d = doublet, t = triplet, q = quartet, br. = broad. [b] Shift values given in ppm. [c] 293 K. [d] 253 K. [e] 266 K. [f] CD<sub>2</sub>Cl<sub>2</sub>. [g] 275 K; data from ref.<sup>[7]</sup>.

observed for 1–6 (see also Scheme 2): Ph'P<sub>A</sub> ↔ Ph'P<sub>B</sub> ↔ Ph'P<sub>C</sub> and Ph''P<sub>A</sub> ↔ Ph''P<sub>B</sub> ↔ Ph''P<sub>C</sub>.

A representative example is reported in Figure 1, in which a section of the <sup>1</sup>H NOESY spectrum of [(triphos)-Rh( $\eta^1$ : $\eta^2$ -P<sub>4</sub>Ph)] (4) clearly displays the exchange peaks between the *ortho*-Ph'P<sub>A</sub> and the *ortho*-Ph'P<sub>B</sub> protons (P1) as well as between the *ortho*-Ph'P<sub>A</sub> and the *ortho*-Ph'P<sub>C</sub> protons (P2).

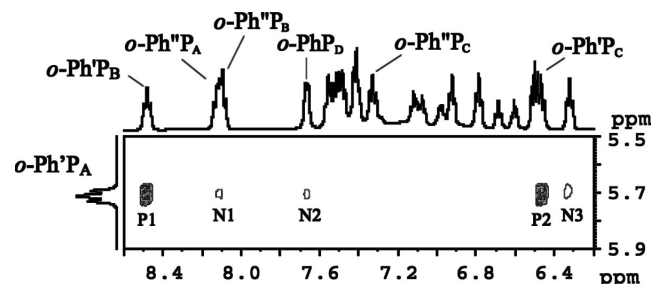


Figure 1. Section of the <sup>1</sup>H NOESY spectrum of [(triphos)-Rh( $\eta^1$ : $\eta^2$ -P<sub>4</sub>Ph)] (4) (500.13 MHz, [D<sub>8</sub>]THF, 266 K,  $\tau_m$  = 1.0 s): positively phased (exchange) cross-peaks are represented by filled circles and negatively phased (NOE) cross-peaks are represented by empty circles. Labels: P1 (*o*-Ph'P<sub>A</sub> – *o*-Ph'P<sub>B</sub>), P2 (*o*-Ph'P<sub>A</sub> – *o*-Ph'P<sub>C</sub>), N1 (*o*-Ph'P<sub>A</sub> – *o*-Ph''P<sub>A</sub>), N2 (*o*-Ph'P<sub>A</sub> – *o*-PhP<sub>D</sub>), N3 (*o*-Ph'P<sub>A</sub> – *m*-Ph'P<sub>A</sub>).

An analogous dynamic behaviour is displayed by the methylenic protons of the triphos chains. In some instances, the rate of the exchange process is faster than the rate of the NOE build-up. This is shown, for example, by the [(triphos)Rh( $\eta^1$ : $\eta^2$ -P<sub>4</sub>PhMe)](OTf) (6) complex in CD<sub>2</sub>Cl<sub>2</sub> solution at 275 K. In fact, the *ortho*-PhP<sub>D</sub> protons show NOE contacts not only with the close *ortho*-Ph'P<sub>A</sub> protons but

also with all the other *ortho* protons exchanging with those of  $\text{Ph}'\text{P}_A$ , namely, the *ortho*- $\text{Ph}'\text{P}_B$  and *ortho*- $\text{Ph}'\text{P}_C$  protons (Figure 2).

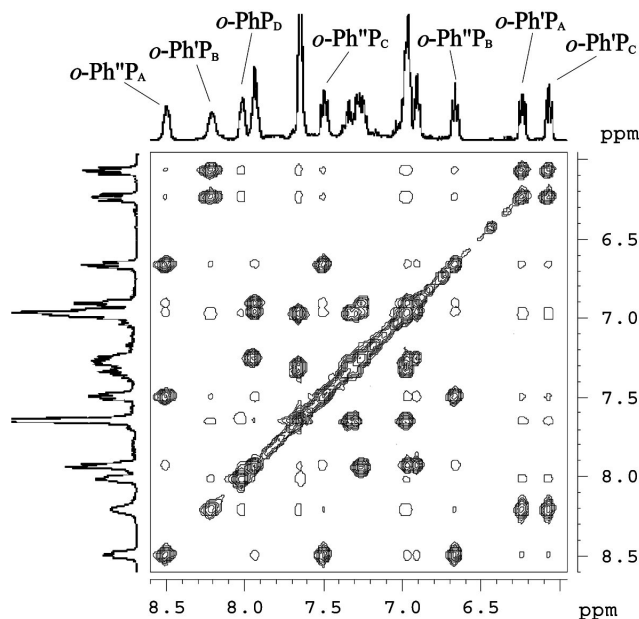


Figure 2. Section of the  $^1\text{H}$  NOESY spectrum of  $[(\text{triphos})\text{-Rh}(\eta^1:\eta^2\text{-P}_4\text{PhMe})](\text{OTf})$  (**6**) in the aromatic region (500.13 MHz,  $\text{CD}_2\text{Cl}_2$ , 275 K,  $\tau_m = 0.8$  s). Positively phased (exchange) cross-peaks are represented by filled circles and negatively phased (NOE) cross-peaks are represented by empty circles.

The presence of a dynamic process in both  $[(\text{triphos})\text{-Rh}(\eta^1:\eta^2\text{-P}_4\text{R})]$  and  $[(\text{triphos})\text{Rh}(\eta^1:\eta^2\text{-P}_4\text{RR}')](\text{OTf})$  complexes was confirmed by 2D  $^{31}\text{P}\{^1\text{H}\}$  EXSY spectroscopy.<sup>[16]</sup> All  $^{31}\text{P}\{^1\text{H}\}$  EXSY spectra are consistent with

the exchange of the phosphorus atoms of triphos. No exchange peaks related to the phosphorus atoms of the  $\text{P}_4$  unit were detected. A section of the  $^{31}\text{P}\{^1\text{H}\}$  EXSY spectrum of **6** is reported in Figure 3 as an example showing the complete network of exchange peaks involving the three triphos P atoms.

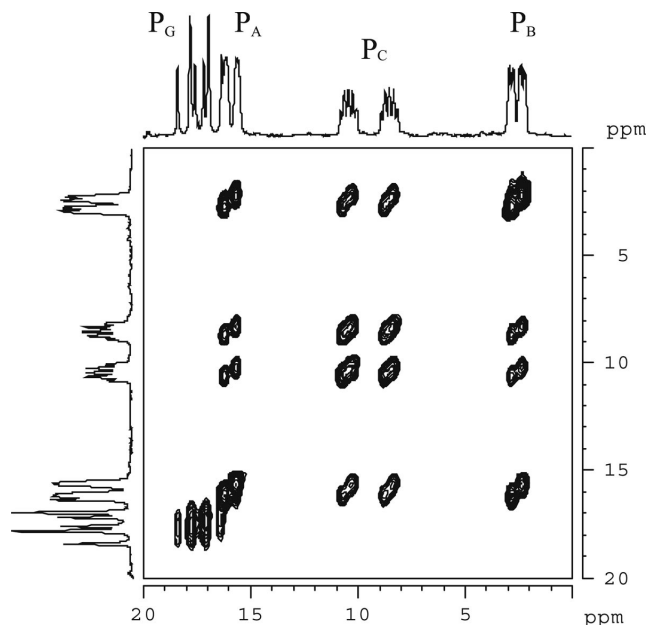


Figure 3. Section of the  $^{31}\text{P}\{^1\text{H}\}$  EXSY spectrum of  $[(\text{triphos})\text{-Rh}(\eta^1:\eta^2\text{-P}_4\text{PhMe})](\text{OTf})$  (**6**) (202.47 MHz,  $\text{CD}_2\text{Cl}_2$ , 275 K,  $\tau_m = 0.1$  s).

The only motion which may account for the observed dynamic behaviour in **1–6** is a slow scrambling of the  $\text{P}_4\text{RR}'$  and (triphos)Rh units with respect to each other. A

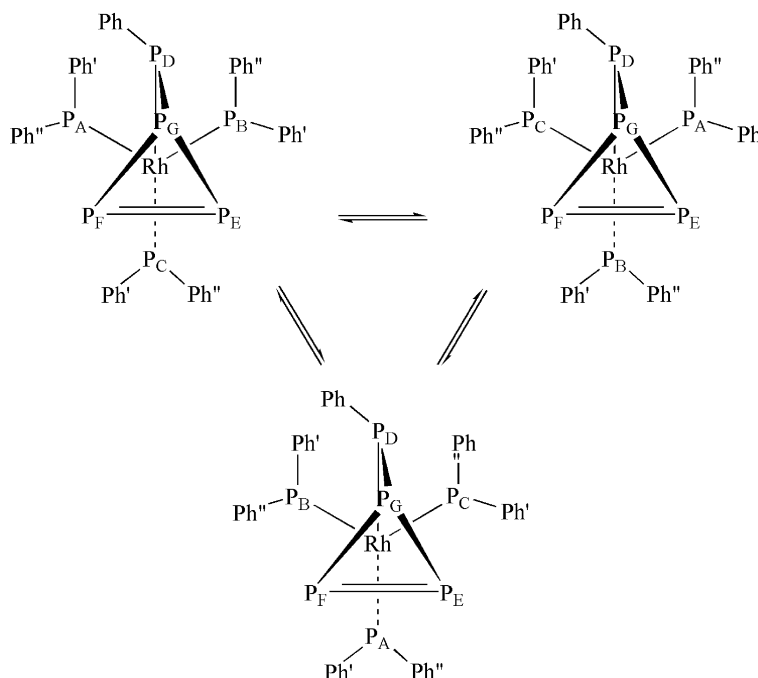


Figure 4. Schematic representation of the dynamic behaviour of  $[(\text{triphos})\text{Rh}(\eta^1:\eta^2\text{-P}_4\text{Ph})]$  (**4**) viewed along the  $\text{Rh-C}(\text{CH}_3)_3$  axis.

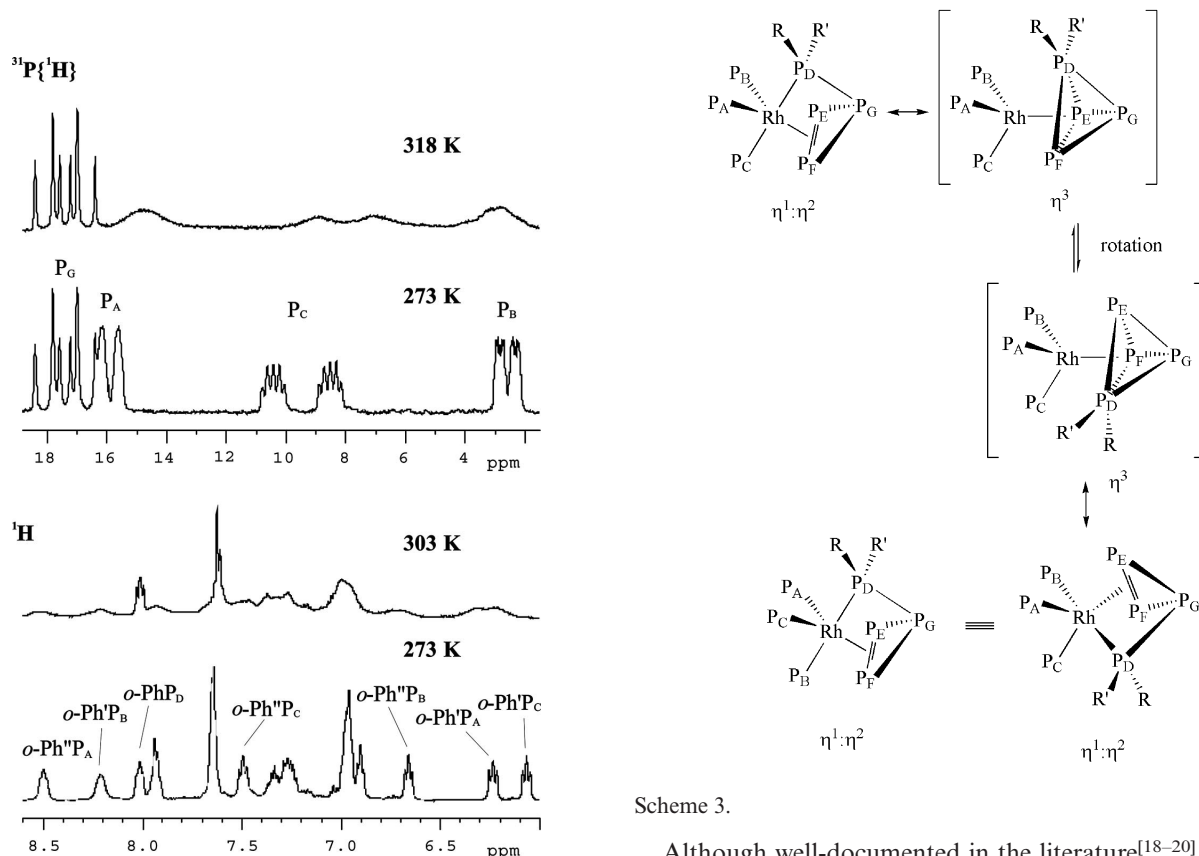
sketch of the proposed motion undergone by these systems is schematically represented in Figure 4 for the neutral [(triphos)Rh( $\eta^1$ : $\eta^2$ -P<sub>4</sub>Ph)] complex (**4**). The process involves the interconversion of three equivalent rotamers by the switching of the phosphorus atom of triphos occupying the *trans*-axial position to the P<sub>D</sub> atom position of the P<sub>4</sub>Ph unit, which is always axial.

To arrive at a better understanding of the observed fluxionality, variable-temperature <sup>1</sup>H and <sup>31</sup>P{<sup>1</sup>H} NMR spectra were recorded for representative complexes over the 273–318 K temperature range in CD<sub>2</sub>Cl<sub>2</sub> solutions. Unfortunately, both because of the decomposition of the complexes at higher temperatures and the lack of appropriate computer programs for the simulation of eight-nuclei spin systems, the activation parameters for the dynamic process could not be determined from conventional line-shape analysis. However, both proton and phosphorus NMR signals show significant temperature-dependent changes. As an example, the <sup>1</sup>H and <sup>31</sup>P{<sup>1</sup>H} NMR spectra in the aromatic and triphos regions for the [(triphos)Rh( $\eta^1$ : $\eta^2$ -P<sub>4</sub>PhMe)]<sup>+</sup> complex (**6**) are reported in Figure 5, respectively. In both spectra, the resonances due to the P<sub>4</sub>PhMe unit (i.e., P<sub>G</sub> and *o*-PhP<sub>D</sub>) sharpen upon increasing the temperature, whereas the resonances due to the triphos nuclei (i.e., P<sub>A</sub>, P<sub>B</sub>, P<sub>C</sub> and their *ortho* protons) broaden and shift toward the coalescence point. These findings are

in line with a rotational exchange involving the triphos nuclei only, as already indicated by the 2D NMR experiments.

### Scrambling Mechanism and DFT (Density Functional Theory) Modelling of the Exchange Process

Different mechanisms to account for the relative motion of the (triphos)Rh and P<sub>4</sub>RR' units in compounds **1–6** can be proposed on the basis of the results of the NMR studies. The dynamic behaviour of the known (triphos)M( $\eta^3$ -P<sub>3</sub>) complexes,<sup>[12,13,17]</sup> which contain the cyclo-P<sub>3</sub> adduct, as well as that of the related carbonyl derivatives—[(triphos)-M{ $\eta^3$ -P<sub>3</sub>[M'(CO)<sub>5</sub>]<sub>x</sub>}] (M = Co, M' = Cr, *x* = 1–3;<sup>[17a,18,19]</sup> M' = Mo, W, *x* = 1;<sup>[19]</sup> 2;<sup>[18]</sup> M = Rh, M' = W, *x* = 1<sup>[19]</sup>), [(triphos)Rh{ $\eta^3$ -P<sub>3</sub>[W(CO)<sub>4</sub>(PPh<sub>3</sub>)]}],<sup>[19]</sup> and [(triphos)-Co{ $\eta^3$ -P<sub>3</sub>[Re(CO)<sub>5</sub>]]]BF<sub>4</sub>,<sup>[19]</sup>—and the intrinsic threefold symmetry of the (triphos)M unit suggest an exchange process involving trihapto-P<sub>3</sub> triangle intermediates which encompass a  $\eta^1$ : $\eta^2 \leftrightarrow \eta^3 \leftrightarrow \text{rotation} \leftrightarrow \eta^3 \leftrightarrow \eta^1$ : $\eta^2$  sequence, as sketched in Scheme 3. Indeed, easy scrambling of the substituted (triphos)M( $\eta^3$ -P<sub>3</sub>) species in solution has been previously reported for the metal carbonyl adducts, [(triphos)M{ $\eta^3$ -P<sub>3</sub>[M'(CO)<sub>4</sub>(L)]<sub>x</sub>}]Y,<sup>[18,19]</sup> and for the di-metallic rhodium–ruthenium species, {[(triphos)Rh]( $\mu$ , $\eta^3$ : $\eta^1$ -P<sub>3</sub>)[CpRu(CH<sub>3</sub>CN)(PR<sub>3</sub>)]}PF<sub>6</sub> (R = Me, Ph, Cy).<sup>[20]</sup>



Scheme 3.

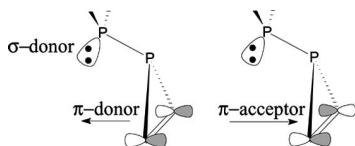
Figure 5. Sections of the variable-temperature NMR spectra of [(triphos)Rh( $\eta^1$ : $\eta^2$ -P<sub>4</sub>PhMe)](OTf) (**6**) recorded at 273 and 318 K (CD<sub>2</sub>Cl<sub>2</sub>). Top: <sup>31</sup>P{<sup>1</sup>H} spectra (202.47 MHz). Bottom: <sup>1</sup>H spectra (500.132 MHz).

Although well-documented in the literature<sup>[18–20]</sup> and attractive for its intrinsic simplicity, the above mechanism seems unlikely in the present case, as it would require several P–P bond-forming/bond-breaking steps within the P<sub>4</sub>RR' unit. This also implies a continuous change of the



metal coordination mode and an energetically expensive sequence of reductive elimination and oxidative addition reactions. Moreover, the trihapto coordination of the ligand would be structurally and electronically inconsistent with a  $P_D$  atom substituted by R and R' groups.<sup>[21]</sup>

If one rules out the mechanism in Scheme 3, only a turnstile process can be invoked.<sup>[22]</sup> Indeed, the (triphos)Rh unit defines a threefold rotor with respect to the  $(\eta^1:\eta^2-P_4RR')$  unit. The turnstile mechanism involves the relative rotation of these two units with respect to each other while maintaining a  $\eta^1:\eta^2$  coordination. In this case, neither cleavage of P–P bonds within the  $P_4$  cage nor a change in the metal oxidation state is required for the rearrangement of the pentacoordinated species. As previously reported,<sup>[7]</sup> the  $P_4RR'$  ligand is able to donate one  $\sigma$  and one  $\pi$  electron pair (Scheme 4). Because of the hybridization of the  $d_\pi$  orbital of the  $L_4M$  fragment,<sup>[23]</sup> the back-donation into the  $P=P$   $\pi^*$  level is greatly favoured when the  $P=P$  double bond lies in the equatorial plane of the TBP.



Scheme 4. Orbital origin of the donor and acceptor capabilities of the  $P_4RR'$  ligands.

The turnstile mechanism requires that the positions of the  $\sigma$  and  $\pi$  electron pairs are switched at some point; that is, the  $P=P$  bond must also be able to occupy the TBP apical position during the interconversion process. The feasibility of such a structural rearrangement is confirmed by the DFT optimization on a model of complex **1** ( $R = H$ ,  $R' =$  lone pair)—namely,  $[(Htriphos)Rh(\eta^1:\eta^2-P_4H)]$ —in which Htriphos is a theoretical counterpart of the real tripodal phosphane with all the phenyl substituents in the ligand replaced with H atoms.<sup>[7]</sup> This model compound is characterized by an actual transition state (one negative frequency for structure **b** in Figure 6), which lies about 20 kcal mol<sup>−1</sup> above the ground state (structure **a** in Figure 6).

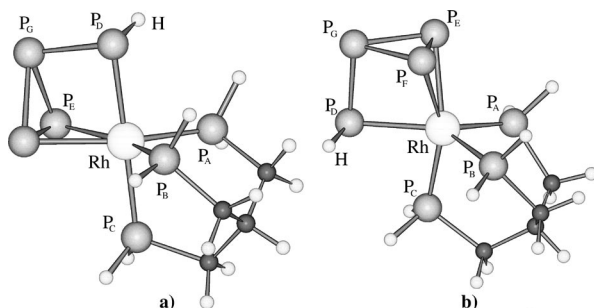


Figure 6. DFT-optimized geometries of the ground state (**a**) and transition state (**b**) of the model compound,  $[(Htriphos)Rh(\eta^1:\eta^2-P_4H)]$ .

The significantly larger stability of the latter structure is due to the metal  $\pi$  back-donation, which occurs when the  $P=P$  bond lies in an equatorial position of the trigonal bipy-

ramidal structure; this is reduced in the apical position. As shown by the distances reported in Table 3, the different conformation has an obvious effect on the geometrical parameters. Thus, in model **b** the  $P=P$  distance is shorter than in **a** (2.14 vs. 2.16 Å, respectively) while the  $Rh-P_E$  and  $Rh-P_F$  bonds are longer (2.53 and 2.52 vs. 2.48 and 2.49 Å, respectively). The relatively high energy barrier for the rearrangement of the whole  $P_4R$  unit with respect to the (triphos)Rh fragment justifies the slow dynamic exchange process observed under the experimental NMR conditions. In fact, the <sup>1</sup>H NOESY and the <sup>31</sup>P{<sup>1</sup>H} EXSY spectra are consistent with a slow scrambling of the  $P_4R$  and (triphos)-Rh units with respect to each other. In conclusion, the reciprocal rearrangement of the bulky threefold and twofold rotors—that is, (triphos)Rh and  $Rh(\eta^1:\eta^2-P_4RR')$ —must be significantly hindered. The situation is fairly similar to  $L_4M(\eta^2\text{-olefin})$  complexes for which comparable rotation barriers are found.<sup>[24]</sup>

Table 3. Selected bond lengths [Å] of the optimized geometries of the ground state (**a**) and transition state (**b**) of the model compound,  $[(Htriphos)Rh(\eta^1:\eta^2-P_4H)]$ .

	Model <b>a</b>	Model <b>b</b>
Rh– $P_A$	2.35	2.35
Rh– $P_B$	2.36	2.36
Rh– $P_C$	2.41	2.30
Rh– $P_D$	2.43	2.51
Rh– $P_E$	2.48	2.52
Rh– $P_F$	2.49	2.53
$P_D$ –H	1.43	1.43
$P_D$ – $P_G$	2.26	2.26
$P_E$ – $P_F$	2.16	2.14
$P_E$ – $P_G$	2.26	2.25
$P_F$ – $P_G$	2.27	2.25

## Conclusions

A detailed multinuclear, multidimensional NMR investigation of both neutral  $\eta^1:\eta^2-P_4R$  and cationic  $\eta^1:\eta^2-P_4RR'$  (triphos)Rh complexes of the general formula  $[(triphos)Rh(\eta^1:\eta^2-P_4RR')]Y_n$  has allowed for a satisfactory structural characterization of the species in solution. Moreover, the fluxional behaviour, which entails the exchange of the triphos phosphorus atoms, has been highlighted. The conclusions are supported by DFT calculations for the  $[(Htriphos)Rh(\eta^1:\eta^2-P_4H)]$  model compound. For this compound, a transition state is detected about 20 kcal mol<sup>−1</sup> above the ground state and this provides a convincing justification for a turnstile pseudorotation process. This implies that the  $P=P$  bond, which belongs to the  $P_3$  triangular face of the  $P_4RR'$  ligand and is coordinated to the metal in a dihapto fashion, switches between the equatorial and axial positions of the bipyramidal geometry. Given the significant energy barrier, the process is hindered and slow, which is fully consistent with the NMR response.

## Experimental Section

**General Data:** The  $[(triphos)Rh(\eta^1:\eta^2-P_4RR')]Y$  [triphos =  $MeC(CH_2PPh_2)_3$ ;  $R = H$ , alkyl, aryl;  $R' =$  lone pair, H, Me] complexes were prepared as previously reported.<sup>[7]</sup>

**NMR Experiments:**  $^{31}\text{P}\{^1\text{H}\}$ ,  $^1\text{H}$  and  $^{13}\text{C}\{^1\text{H}\}$  NMR spectra were recorded with a Bruker Avance DRX-500 spectrometer equipped with a variable-temperature control unit accurate to  $\pm 0.1^\circ\text{C}$  and operating at 202.47, 500.13 and 125.76 MHz, respectively; deuterated solvents dried with molecular sieves (4 Å) were used.  $^{31}\text{P}\{^1\text{H}\}$  chemical shifts are reported relative to external 85%  $\text{H}_3\text{PO}_4$ , with downfield values reported as positive.  $^1\text{H}$  and  $^{13}\text{C}\{^1\text{H}\}$  chemical shifts are reported relative to tetramethylsilane as an external reference and were calibrated against the residual solvent resonance ( $^1\text{H}$ ) or the deuterated solvent multiplet ( $^{13}\text{C}$ ). The assignments of the signals resulted from 1D spectra, 2D  $^1\text{H}$  DQF-COSY,  $^{31}\text{P}\{^1\text{H}\}$  COSY,  $^1\text{H}$  NOESY and proton-detected 2D  $^1\text{H}$ - $^{13}\text{C}$  and  $^1\text{H}$ - $^{31}\text{P}$  correlations. 2D NMR spectra were recorded with degassed non-spinning samples by using pulse sequences suitable for phase-sensitive representations and by using TPPI. Standard pulse sequences were used for the  $^1\text{H}$  NOESY<sup>[14]</sup> experiments: 1024 increments 2 K in size (with 8 scans each) and covering the full range in both dimensions (ca. 5000 Hz) were acquired with a relaxation delay of 2 s and a mixing time of 1.0 or 0.8 s. The 2D  $^{31}\text{P}\{^1\text{H}\}$  EXSY<sup>[16]</sup> spectra were recorded using the NOESY pulse sequence<sup>[14b,25]</sup> with  $^1\text{H}$  decoupling during acquisition: 1024 increments 2 K in size (with 64 scans each) and covering the full range in both dimensions were collected with a relaxation delay of 0.8 s and mixing times of 0.10, 0.50, 0.80 and 1.00 s.

**Computational Studies:** Structural optimizations were carried out at the hybrid density functional theory (DFT) using the Gaussian98 program.<sup>[26]</sup> The triphos ligand was modelled by replacing all of the phenyl substituents with H atoms (Htriphos). This allows for the maintenance of the typical geometric constraints at the metal. In particular, the three P-Rh-P angles are forced to be almost  $90^\circ$ . The method used was the Becke three-parameter hybrid exchange-correlation functional containing the Lee, Yang and Parr nonlocal gradient correction (B3LYP).<sup>[27,28]</sup> The nature of the optimized structures was confirmed by calculation of the frequencies. The basis set for the Rh atom utilized the effective core potentials of Hay and Wadt with the associated double- $\zeta$  valence basis functions.<sup>[29]</sup> The basis set used for the remaining atomic species was 6-31G(d,p).<sup>[30]</sup> The geometrical parameters for the minimum structure of model **a** (see text above) were compared with the X-ray solid-state features of  $[(\text{triphos})\text{Rh}(\eta^1\text{-}\eta^2\text{-P}_4\text{PhMe})](\text{OTf})$ <sup>[7]</sup> and indicate a good agreement between the two structures.

## Acknowledgments

The authors are thankful for the support of the European Community through the FP6 IDECAT Network of Excellence (contract NMP3-CT-2005-011730). AI and CM are grateful for the computing time provided by CINECA under the agreement of the National Council for Research (CNR). Thanks are also given to Thermphos Intl., Vlissingen, NL for a generous loan of white phosphorus and for supporting this research activity.

- [1] a) D. E. C. Corbridge, *Phosphorus. An Outline of its Chemistry, Biochemistry and Technology*, 5<sup>th</sup> ed., in *Studies in Inorganic Chemistry*, vol. 20, Elsevier, Amsterdam, **1995**; b) J. Emsley, *The 13<sup>th</sup> Element: The Sordid Tale of Murder, Fire, and Phosphorus*, Wiley, New York, **2002**.
- [2] M. Peruzzini, L. Gonsalvi, A. Romerosa, *Chem. Soc. Rev.* **2005**, 34, 1038.
- [3] a) M. Peruzzini, I. de los Rios, A. Romerosa, F. Vizza, *Eur. J. Inorg. Chem.* **2001**, 593; b) M. Ehses, A. Romerosa, M. Peruzzini, *Top. Curr. Chem.* **2002**, 220, 108; c) M. Peruzzini, R. R. Abdeimova, Y. Budnikova, A. Romerosa, O. J. Scherer, H. Sitzmann, *J. Organomet. Chem.* **2004**, 689, 4319.
- [4] J. D. Masuda, W. W. Schoeller, B. Donnadieu, G. Bertrand, *Angew. Chem. Int. Ed.* **2007**, 46, 7052.
- [5] M. Peruzzini, J. A. Ramirez, F. Vizza, *Angew. Chem. Int. Ed.* **1998**, 37, 2255.
- [6] P. Barbaro, M. Peruzzini, J. A. Ramirez, F. Vizza, *Organometallics* **1999**, 18, 4237.
- [7] P. Barbaro, A. Ienco, C. Mealli, M. Peruzzini, O. J. Scherer, G. Schmitt, F. Vizza, G. Wolmershäuser, *Chem. Eur. J.* **2003**, 9, 5195.
- [8] The  $[(\text{triphos})\text{Rh}(\eta^1\text{-}\eta^2\text{-P}_4\text{R})]$  complexes react with hydrogen to form phosphane,  $\text{PH}_3$ , or primary phosphanes,  $\text{PH}_2\text{R}$  (R = alkyl, aryl). While the yield of  $\text{PH}_3$  is almost quantitative, primary phosphanes are never produced in yields higher than 15%.
- [9] See for example: M. Scheer, E. Leiner, P. Kramkowski, M. Schiffer, G. Braum, *Chem. Eur. J.* **1998**, 4, 1917.
- [10] See for example: O. J. Scherer, G. Berg, G. Wolmershäuser, *Chem. Ber.* **1996**, 129, 53.
- [11] See for example: O. J. Scherer, B. Werner, G. Heckmann, G. Wolmershäuser, *Angew. Chem. Int. Ed. Engl.* **1991**, 30, 553.
- [12] M. Di Vaira, L. Sacconi, *Angew. Chem. Int. Ed. Engl.* **1982**, 21, 330.
- [13] M. Di Vaira, P. Stoppioni, M. Peruzzini, *Polyhedron* **1987**, 6, 351.
- [14] a) V. Sklener, H. Miyashiro, G. Zon, H. T. Miles, A. Bax, *FEBS Lett.* **1986**, 208, 94; b) J. Jeener, B. H. Meier, P. Bachmann, R. R. Ernst, *J. Chem. Phys.* **1979**, 71, 4546.
- [15] W. E. Hull, *Methods in Stereochemical Analysis in Two-Dimensional NMR Spectroscopy Applications for Chemists and Biochemists* (Eds.: W. R. Croasum, R. M. K. Carlson), VCH, Weinheim, Germany, **1994**, chapter 2, pp. 327–333.
- [16] A. Bax, *Two-Dimensional Nuclear Magnetic Resonance in Liquids*, Delft University Press, Dordrecht, The Netherlands, **1982**.
- [17] a) M = Co: C. A. Ghilardi, S. Midollini, L. Sacconi, *Inorg. Chem.* **1980**, 19, 301; b) M = Rh, Ir: C. Bianchini, C. Mealli, A. Meli, L. Sacconi, *Inorg. Chim. Acta* **1979**, 37, L543.
- [18] M. Di Vaira, M. Ehses, M. Peruzzini, P. Stoppioni, *J. Organomet. Chem.* **2000**, 593–594, 127.
- [19] M. Di Vaira, M. Ehses, M. Peruzzini, P. Stoppioni, *Inorg. Chem.* **2000**, 39, 2199.
- [20] P. Barbaro, M. Di Vaira, M. Peruzzini, S. Seniori Costantini, P. Stoppioni, *Eur. J. Inorg. Chem.* **2005**, 1360.
- [21] Also, for  $\text{P}_4$  metal complexes,<sup>[2]</sup>  $\eta^3$ -coordination has not yet been reported. Remarkably, while the intact *tetrahedro*-tetraphosphorus molecule,  $\text{P}_4$ , may coordinate a transition metal fragment either as a  $\eta^1$ - or  $\eta^2$ -ligand,<sup>[2]</sup> no example of  $\eta^3$ -coordination is known. The latter was calculated to be energetically disfavoured for  $[(\text{PPh}_3)_2\text{ClRh}(\text{P}_4)]$  with respect to  $\eta^2$ - and  $\eta^1$ -coordination modes. See: S.-W. Kang, T. A. Albright, J. Silvestre, *Croat. Chem. Acta* **1984**, 57, 1355.
- [22] M. E. Cass, K. K. Hii, H. S. Rzepa, *J. Chem. Educ.* **2006**, 83, 336.
- [23] T. A. Albright, J. K. Burdett, M. H. Whangbo, *Orbital Interactions in Chemistry*, Wiley, New York, **1985**.
- [24] R. Hoffmann, *Science* **1981**, 211, 995.
- [25] R. Benn, H. Günther, *Angew. Chem. Int. Ed. Engl.* **1983**, 22, 350.
- [26] M. J. Frisch, G. W. Trucks, H. B. Schlegel, G. E. M. Scuseria, A. Robb, J. R. Cheeseman, V. G. Zakrzewski, J. A. Montgomery, R. E. Stratmann, J. C. Burant, S. Dapprich, J. M. Millam, A. D. Daniels, K. N. Kudin, M. C. Strain, O. Farkas, J. Tomasi, V. Barone, M. Cossi, R. Cammi, B. Mennucci, C. Pomelli, C. Adamo, S. Clifford, J. Ochterski, G. A. Petersson, P. Y. Ayala, Q. Cui, K. Morokuma, D. K. Malick, A. D. Rabuck, K. Raghavachari, J. B. Foresman, J. Cioslowski, J. V. Ortiz, B. B. Stefanov, G. Liu, A. Liashenko, P. Piskorz, I. Komaromi, R. Gomperts, R. L. Martin, D. J. Fox, T. Keith, M. A. Al-Laham, C. Y. Peng, A. Nanayakkara, C. Gonzalez, M. Challacombe, P. M. W. Gill, B. G. Johnson, W. Chen, M. W. Wong, J. L.

- Andres, M. Head-Gordon, E. S. Replogle, J. A. Pople, *Gaussian 98*, Revision A.9, Gaussian Inc., Pittsburgh, PA, **1998**.
- [27] A. D. Becke, *J. Chem. Phys.* **1993**, 98, 5648.
- [28] C. Lee, W. Yang, R. G. Parr, *Phys. Rev.* **1998**, B37, 785.
- [29] P. J. Hay, W. R. Wadt, *J. Chem. Phys.* **1985**, 82, 299.
- [30] P. C. Hariharan, J. A. Pople, *Theor. Chim. Acta* **1973**, 28, 213.

Received: October 4, 2007

Published Online: January 15, 2008